

Enhancement of electron-hole pair mobilities in thin GaAs/Al_xGa_{1-x}As quantum wells

H. Hillmer*

Deutsche Bundespost TELEKOM, Forschungsinstitut beim FTZ, Postfach 10 00 03, D-6100 Darmstadt, Federal Republic of Germany

A. Forchel

Technische Physik, Universität Würzburg, Am Hubland, D-8700 Würzburg, Federal Republic of Germany

C. W. Tu[†]

AT&T Bell Laboratories, Murray Hill, New Jersey 07974-2070

(Received 20 June 1991)

We have investigated the lateral transport of excitons and free carriers in thin GaAs/Al_xGa_{1-x}As quantum wells over a wide temperature range, between 10 and 230 K. For all temperatures we observe an increase of the ambipolar diffusivities with increasing well widths. According to different transport phenomena, the entire temperature range can be divided into three parts. For $40 < T < 180$ K, we obtain an isothermal diffusion for the lateral motion of excitons. The experimental data can quantitatively be explained by the contributions of different scattering mechanisms: interface-roughness, barrier-disorder-alloy, acoustic-deformation-potential, and polar-optical-phonon scattering. Raising the temperature in the range $180 < T < 230$ K, we find an unexpected increase of the diffusivities for small well widths (below 5 nm). This can be described by the thermal dissociation of excitons into free carriers revealing higher diffusivities. For decreasing temperatures in the range $10 < T < 40$ K, we observed considerably enhanced diffusivities in thin quantum wells. We attribute this to locally elevated phonon populations or temperature gradients in the optically excited sample volume.

Carrier transport studies probing the carrier motion by time-of-flight (TOF) arrangements require high spatial and temporal resolution. In vertical TOF experiments a high spatial resolution can be obtained by using specific probe layers, e.g., quantum wells^{1,2} (QW's) embedded in the sample structure. The transport distance can be either determined by two different QW's (Ref. 1) or by the sample surface and a single QW.^{2,1} In high-resolution lateral TOF studies the flight distance can be defined by opaque masks with transparent windows³ or holes⁴⁻⁷ which are placed on the semiconductor surface.

In this paper the lateral motion of ambipolar carrier systems (excitons and free carrier pairs) is studied over a wide temperature range (10–230 K). Within this range we emphasize the study of carrier mobilities and diffusivities at low and high temperatures. Compared to theoretical predictions uniquely based on a single carrier species, a uniform lattice temperature and different scattering mechanisms, the experimental data at low and high temperatures yield considerably larger values. In the high-temperature range this diffusivity increase is found to be most probably due to thermal dissociation of excitons into free carrier pairs. At low temperatures the unexpected large diffusivities are related to nonequilibrium effects in the electronic and lattice system.

As described elsewhere,⁴⁻⁷ a sample-mask combination was used for the experiments. The masks contain circular areas (holes) which are transparent for both the laser excitation light and the luminescence of the QW's. We used a hole radius of 2 μm which is comparable to the carrier diffusion length. By short dye laser pulses (~8 ps) carrier pairs were generated in the QW inside the

hole defined by the mask. For relatively low carrier densities the radiative recombination is proportional to the carrier concentration and is used to probe the lateral carrier motion in different QW's. Recording the QW emission as a function of time, the evolution of the carrier concentration in the hole area can be observed. Carriers under opaque parts of the mask during their lifetime do not contribute to the detectable emission. Therefore, the time-resolved emission from the hole area includes information about important transport properties like the diffusivity and the mobility. These quantities can be determined by the evaluation of the measured temporal intensity variation as a function of both temperature and well width. For the experiments the samples are mounted in a variable-temperature Dewar (10–300 K). The emission is dispersed by a double monochromator, detected by a fast microchannel plate photomultiplier, and processed by a photon-counting system (total time resolution ≈ 50 ps). A detailed description of our TOF method and the experimental setup is given in Ref. 5.

The radiative emission of the $n=1$ transition in the QW's as a function of time shows a fast increase within several ps and a considerably longer decay. By using our TOF configuration the temporal variation of the emission intensity includes information about the carrier lifetime and the diffusivity (for details see, e.g., Ref. 5). These time-resolved luminescence profiles are recorded first without mask to determine the exciton lifetime as a function of QW width and temperature. In these studies the emission decay is determined only by the carrier lifetime. Second, using masks of 2-μm-hole radius the decay of the recorded emission is considerably shortened compared to

simple lifetime measurements, since in addition to recombination the decay is strongly enhanced by carrier transport under masked sample parts. The faster the lateral carrier motion, the more carriers can reach covered sample parts and the larger the difference in the decay between the emission profiles detected with and without masks.^{5,7} To evaluate the experimental profiles we use the two-dimensional (2D) diffusion equation which contains the diffusivity D and a linear recombination term characterized by the radiative lifetime τ :

$$\frac{\partial c}{\partial t} = D \left[\frac{\partial^2 c}{\partial x^2} + \frac{\partial^2 c}{\partial y^2} \right] - \frac{c}{\tau}. \quad (1)$$

This equation is solved numerically with respect to the initial condition. The diffusivity is the only free parameter in this equation since the lifetime is measured separately without mask coverage.

By fitting the theoretical profiles to the experimental curves we are able to precisely determine the diffusivity as a function of temperature and well width.^{4,5} In the temperature range between 40 and 180 K the experimental profiles can perfectly be described by the theory based on the diffusion equation demonstrating the isothermal lateral carrier diffusion. For low carrier densities the ambipolar carrier system is almost entirely in the excitonic phase in this temperature range.

The diffusivities obtained for a GaAs/Al_{0.37}Ga_{0.63}As sample containing QW's of $L_z = 1.5, 2.5, 5,$ and 10 nm well width are depicted in Fig. 1 as a function of temperature. We observe a strong dependence of the diffusivities on temperature, increasing up to about 100 K and decreasing again at higher temperatures. A strong dependence on well width is found in addition to this temperature dependence. With increasing L_z the diffusivities considerably rise over the entire temperature range which is found to be strongest for low temperatures. The shape (slopes, widths) and the shift of the maximum of the $D(T, L_z)$ data is governed by the interaction of various scattering mechanisms which have a different dependence on well width and temperature. The shift of the maximum is mainly due to the interaction of acoustic-deformation-potential scattering, barrier-alloy-disorder scattering, and polar-optical-phonon scattering. A similar variation of the diffusivities $D(T, L_z)$ was also obtained in samples with an aluminum content of 0.3, 0.5, and 1.0. For a given aluminum mole fraction we found no overcrossing of the $D(T)$ profiles for different L_z .

For the low exciton densities considered here the diffusivities $D(L_z, T)$ can be converted into mobilities $\mu(L_z, T)$ using the Einstein relation $\mu(L_z, T) = D(L_z, T)e/(kT)$. For $80 \lesssim T < 180$ K the variation with temperature and well width can quantitatively be described in our calculations by barrier-alloy-disorder scattering and acoustic-deformation-potential scattering. For $T > 180$ K polar-optical-phonon scattering also contributes and dominates the mobilities for increasing temperature. The discussion of the contribution of the different scattering mechanisms will be the subject of a forthcoming publication.

In the low-temperature region ($40 < T \lesssim 80$ K) the ob-

served strong well-width dependence quantitatively can be attributed to efficient interface-roughness scattering.⁸⁻¹⁰ Our interface roughness model used for the characterization of the interface morphology contains two variable parameters: an average terrace height and an average terrace length. Since the interface roughness strongly influences both lateral mobilities and linewidths of photoluminescence spectra, the average terrace length and height simultaneously have to describe the experimental mobility and linewidth data for all temperatures. For $T = 10$ K and QW widths of $L_z = 1.5, 2.5, 5,$ and 10 nm, we have observed linewidths of 6.2, 2, 1, and 0.9 meV, respectively. For a given QW width we have varied the average length and height in our model to obtain the best description of all experimental data by curve fitting. In the low temperature range interface-roughness scattering dominates, but acoustic-deformation-potential scattering and barrier-alloy-disorder scattering also contribute and have to be considered if the experimental mobility data are used to determine the parameters included in our interface-roughness model. Thus, according to Matthiessen's rule the inverse experimental mobility $(\mu_{\text{expt}})^{-1}$ has to be approximated by the sum of the inverse mobilities of interface-roughness scattering (ir), acoustic-deformation-potential scattering (ac) and barrier-alloy-disorder scattering (bal):

$$\frac{1}{\mu_{\text{expt}}} = \frac{1}{\mu_{\text{ir}}} + \frac{1}{\mu_{\text{ac}}} + \frac{1}{\mu_{\text{bal}}}. \quad (2)$$

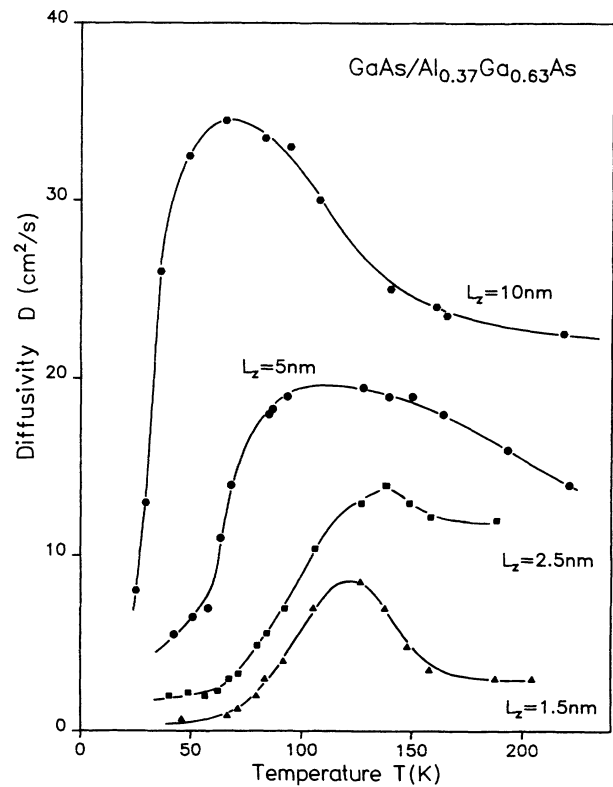


FIG. 1. Diffusivities of two-dimensional excitons determined by the method of transparent hole area as a function of temperature for different well widths. The solid lines are drawn to guide the eye.

From the formula given in Ref. 5 the mobilities μ_{ac} and μ_{bal} can be calculated. Thus, we determine the mobility μ_{ir} from Eq. (2) in the low-temperature range and fit this quantity by calculations based on our interface-roughness model. For the sample with an aluminum content of 0.37 we obtain an average step height of one monolayer for all QW widths and an average terrace length increasing from 2 to 8 nm for L_z rising from 1.5 to 10 nm, respectively. These values are comparable to those reported in Refs. 8–10. However, the increase of the average terrace length with rising well width is an interesting new result which we also found in samples having an aluminum content of 0.3 and 0.5. Note that in our calculation the variation of the interface-roughness scattering with temperature is included. In contrast, this temperature dependence was neglected in the calculations of Refs. 8 and 9 since these experiments were performed at helium temperatures, which justifies the use of the Fermi distributions of $T=0$.

The terrace sizes obtained by the evaluation of mobility data and photoluminescence linewidths are further consistent with the single emission lines observed for each QW in the photoluminescence spectra. Since the lateral extension of the excitons is larger than the terrace lengths, the exciton averages over details in the interface morphology within a lateral area roughly defined by the exciton extension. This causes the observed interface-roughness broadening of the emission lines in the spectra. In contrast sharp photoluminescence lines emitted from QW areas having pseudomonolayer flat interface islands can be observed if the size of the island by far exceeds the lateral exciton extensions.^{11,7}

In the following we study more complicated transport phenomena. In the low-temperature range ($10 < T < 40$ K) our model will approximate exciton diffusion and nonequilibrium effects in the carrier and phonon system. In the high-temperature range ($180 < T < 230$ K) our model will yield diffusivities averaged over the contribution of two different particle species (excitons and free carriers).

For a single particle species with a given effective mass and a carrier temperature close to the uniform lattice temperature the sum of different scattering mechanisms according to Matthiessen's rule predicts a mobility or the diffusivity decreasing monotonically with increasing temperature. However, for small well widths and $T > 160$ K our studies provide a different behavior which is depicted in Fig. 2. The experimentally obtained curvature ($\partial^2 D / \partial T^2 > 0$) and the reincrease for $T > 160$ K indicates that the transport cannot entirely be described within the model of isothermal diffusion of excitons with the above scattering mechanisms. We have obtained a similar result in growth interrupted thin QW's. The unexpected increase of the diffusivity starts at temperatures where the thermal energy (kT) reaches the magnitude of the exciton binding energy. Therefore, we presume that the increase of the diffusivity with rising temperature probably indicates the growing dissociation rate of excitons into free carriers. This qualitative estimate will be confirmed below by a more quantitative description.

According to our calculation for acoustic-

deformation-potential scattering, we obtain for free carriers a less efficient scattering compared to excitons.⁵ Hence, excitons are less mobile than free carriers, if acoustic-deformation-potential scattering dominates. With rising temperature the exciton concentration decreases due to thermal dissociation of excitons and the free carrier concentration accordingly increases. Thus, the increase of the diffusivities is most probably due to the phase transition between the excitons and free carriers revealing different mobilities. We have demonstrated in Ref. 5 that acoustic-deformation-potential scattering limited mobility is proportional to L_z/T for 2D excitons and free carrier pairs. However, the absolute values of free carrier pairs exceed those of excitons by more than one order of magnitude.⁵

Figure 3 compares model calculations with the measured diffusivities (symbols) for $L_z = 1.5$ nm and $L_z = 2.5$ nm in the left- and right-hand parts of the diagram, respectively. In the lower temperature range of the diagram the majority of the carriers will be excitons. Hence, the excitonic acoustic-deformation-potential limited diffusivity (ac, exc., full line) will dominate the scattering process by acoustic phonons. In contrast, in the high-temperature range of the diagram the number of free carriers considerably increase. Thus, at higher temperatures the ambipolar acoustic-deformation potential limited diffusivity (ac, amb., solid line) is expected to dominate the scattering process by acoustic phonons. Further-

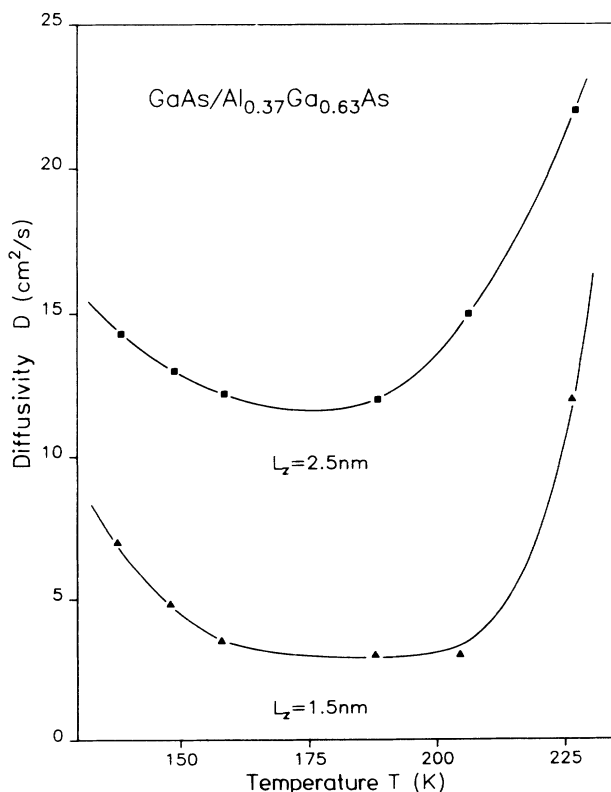


FIG. 2. Experimental diffusivities for higher temperatures given for two different well widths as a function of temperature. The solid lines are drawn to guide the eye.

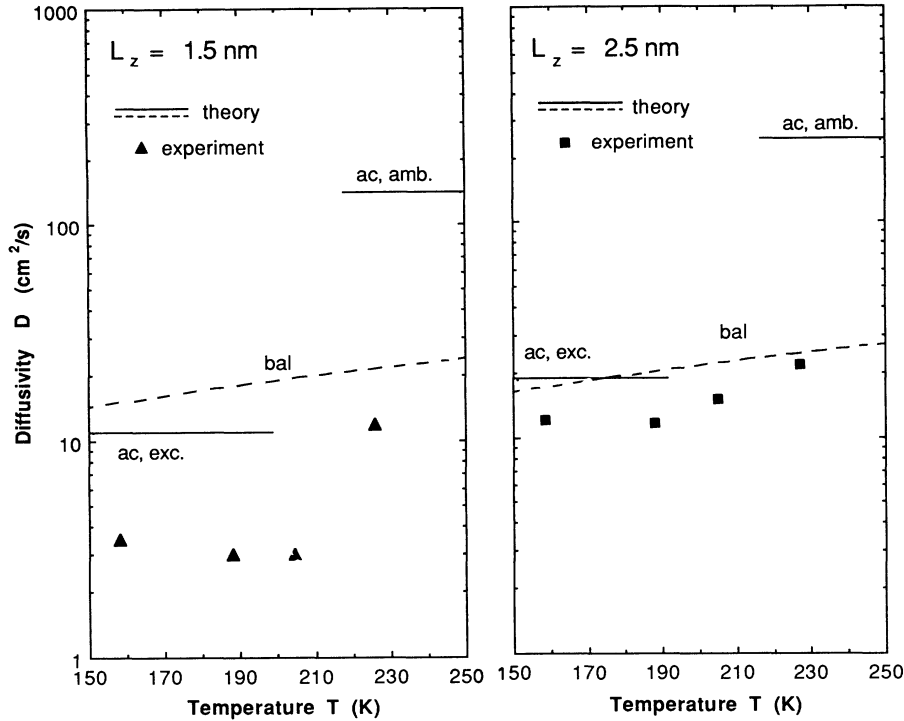


FIG. 3. Diffusivities for high temperatures together with different theoretical approaches (solid and broken lines). The broken line indicates the temperature variation of the diffusivities limited by barrier-alloy-disorder scattering (bal). The diffusivity limited by acoustic-deformation-potential scattering (solid lines) is calculated for excitons (ac, exc.) and free ambipolar carriers (ac, amb.). The left and right parts of the diagram depict the results for well widths of 1.5 and 2.5 nm, respectively.

more, the contribution of the well-width dependent barrier-alloy-disorder scattering⁵ (broken line) is included in both diagrams. Since the acoustic-deformation-potential scattering limited mobilities are proportional to L_z/T , the respective diffusivities are independent of temperature, according to the Einstein relation, as indicated in Fig. 3. The absolute values of the different scattering contributions as well as their variation with temperature indicate that the dissociation of excitons into free carriers most probably is responsible for the increase of the diffusivities observed in the experiment.

Since the contributions of further scattering mechanisms such as polar-optical-phonon scattering show a much weaker dependence on well width, the absolute change in the diffusivity is strongest for small diffusivities, i.e., small well widths where the acoustic-deformation-potential scattering dominates (see Fig. 3 and Ref. 5). Thus, for larger well widths (e.g., ≈ 5 nm) we observe no increase in the diffusivities with rising temperature for $T > 160$ K. In this case the exciton dissociation will not significantly influence the diffusivities via the change in the deformation-potential scattering rate. This experimental observation is a further proof for our interpretation that the increase of the diffusivities at higher temperatures is due to exciton dissociation.

Using a system of rate equations to determine the variation of exciton and free electron-hole pair concentrations with temperature we can calculate the change of the measured diffusivity with temperature. In this model ex-

citon dissociation into free carrier pairs, exciton formation from free carriers, exciton recombination, free carrier pair recombination, and interface recombination are taken into account. The considered scattering mechanisms are acoustic-deformation-potential scattering, barrier-alloy-disorder scattering, and polar-optical-phonon scattering. These model calculations including no free parameters yield a good agreement with the measured variation of the diffusivity with temperature (Fig. 2) and will be published elsewhere. This calculation is an improvement of the preliminary theoretical description shown in Fig. 3. A comparison in this temperature range between samples grown under continuous and interrupted growth conditions will also be the subject of a forthcoming publication.

In addition to the high-temperature range we observe in our experiment an unexpected temperature variation of the diffusivities also below 40 K. According to Fig. 4 the diffusivities again increase with decreasing temperature for $T < 40$ K and we obtain $(\partial^2 D / \partial T^2) > 0$ also in this temperature range. Hence, the description of the lateral motion seems to be incomplete and the evaluation by our model is an approximation in this temperature range.

In the low-temperature region a quantitative description of the diffusivity increase with decreasing temperature is currently not available. The unexpected temperature variation of the diffusivity might be due to the following reasons: Since the carriers are optically generated

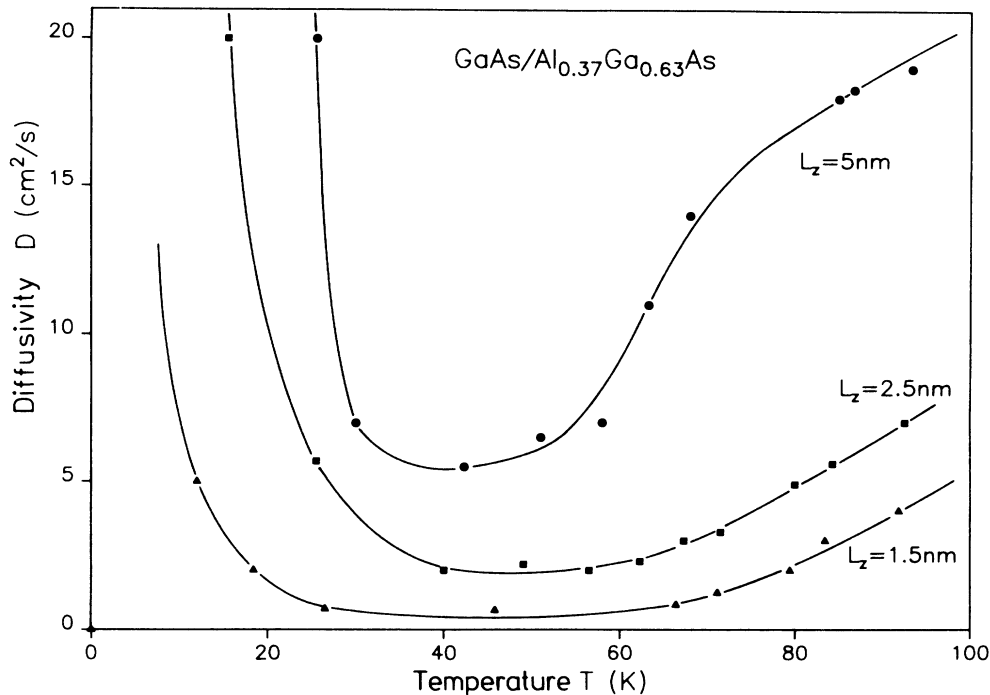


FIG. 4. Experimental diffusivities for low temperatures given for three different well widths as a function of temperature. The solid lines are drawn to guide the eye.

at relatively high excess energies the carrier relaxation and thus phonon emission will lead to an energy transfer from the carrier system to the lattice inside the generation volume. The transferred energy per scm^2 is nearly independent of the lattice temperature and may lead to a small but noticeable increase in the lattice temperature inside the generation volume. This will result in temperature gradients in the 2D layer in radial directions. In addition to the exciton diffusion due to the lateral carrier density gradient a small contribution of thermodiffusion¹² may thus be possible. In addition to thermodiffusion the observed reincrease in the diffusivities may also be influenced by ballistic parts in the lateral transport.

Immediately after the optical excitation optical phonons are generated by the carrier energy relaxation. This provides a nonequilibrium population of optical phonon modes¹³ during a short time interval.¹⁴ After a short time the optical phonons decay into acoustic phonons.¹⁵ However, due to the phonon dispersion relation acoustic phonons have considerably high group velocities, i.e., they are much less localized compared to optical phonons. Therefore, the localized generation of optical phonons indirectly leads to a directed motion of acoustic phonons in radial direction. In 3D systems this phenomenon is called "phonon wind"¹⁶⁻¹⁸ which may push the excitons in addition to the diffusion. In this case the acoustic phonons interact with the excitons via the deformation potential and mainly exchange momentum. Such an effect may also exist in 2D carrier systems and may be partly responsible for the observed enhanced low-temperature diffusivities in our studies. An increase in the diffusivity with decreasing temperature was reported in the temper-

ature range between 12 and 25 K, for electron-hole plasma in GaAs/ $\text{Al}_x\text{Ga}_{1-x}\text{As}$ QW structures¹⁸ and referred to phonon wind. Increasing the laser power we obtain higher diffusivities in the evaluation of our transport experiments. All processes referred in this paragraph (except the possible ballistic contribution) are consistent with this observed dependence on laser power.

Since in our QW samples the exciton extension exceeds typical interface roughness terrace lengths (see above) the QW emission lines will not shift energetically during the exciton lifetimes. In contrast, in samples which have a larger scale interface roughness (more extended terraces or islands)⁷ a carrier diffusion and relaxation into these islands may cause a shift of the whole QW emission lines to lower energies during the exciton lifetime at low temperatures.¹⁹ Due to the short terrace lengths ($\Lambda \sim 2$ nm for $L_z = 1.5$ nm and $\Lambda \sim 2.6$ nm for $L_z = 2.5$ nm) we believe that such processes cannot cause the strong increase of the diffusivities at low temperatures.

As shown in Figs. 1, 2, and 4 we obtain for all temperatures an increase in the diffusivities with increasing well width. Remarkably no overcrossing between $D(T)$ curves of different well widths occurs in the total temperature range between 10 and 230 K despite numerous points of inflexion.

In addition to the results of GaAs QW's discussed here, we also observed enhanced mobilities for low temperatures in $\text{In}_{0.53}\text{Ga}_{0.47}\text{As}/\text{InP}$ QW's. The mobilities strongly increase with decreasing temperature for $10 \leq T \leq 30$ K. Similar to the GaAs case locally elevated phonon population, directed acoustic-phonon motion, or temperature gradients may be responsible for the ob-

served behavior in this material system.

In conclusion, we have observed an increase in the ambipolar diffusivities with rising well widths in the entire studied temperature range of $10 < T < 230$ K. No overcrossing between the variations of the diffusivities with varying temperature occurs for different well widths. According to our results we have divided the entire temperature range into three parts revealing different transport behavior. (i) For $40 < T < 180$ K the experimental data can be quantitatively explained by different scattering mechanisms (interface-roughness, barrier-disorder-alloy, acoustic-deformation-potential, and polar-optical-phonon scattering). (ii) $180 < T < 230$ K: with rising temperature we observe an unexpected reincrease in the diffusivities for small well widths (below 5 nm). This can quantitatively be described by the growing thermal dissociation of

excitons into free carriers. (iii) $10 < T < 40$ K: for decreasing temperatures we found a growing diffusivity in thin GaAs/Al_xGa_{1-x}As and In_{1-y}Ga_yAs/InP QW's. This effect may be due to locally enhanced phonon population, or temperature gradients may be responsible.

We would like to thank M. Pilkuhn, R. Sauer, S. Hansmann, and M. Morohashi for stimulating discussions and B. Hillmer for experimental assistance. The experimental work has been performed at 4. Physikalisches Institut, Universität Stuttgart, D-7000 Stuttgart, Federal Republic of Germany. The financial support by the Deutsche Forschungsgemeinschaft (SFB 329) and the Stiftung Volkswagenwerk is gratefully acknowledged.

*Present address: NTT, Opto-Electronics Laboratories, 3-1 Morinosato Wakamiya, Atsugi-shi, 243-01 Japan.

†Present address: Department of Electrical and Computer Engineering, University of California, San Diego, La Jolla, CA 92093-0407.

¹H. Hillmer, G. Mayer, A. Forchel, K. S. Löchner, and E. Bauser, *Appl. Phys. Lett.* **49**, 948 (1986); H. Hillmer, A. Forchel, T. Kuhn, G. Mahler, and H. P. Meier, *Phys. Rev. B* **43**, 13 992 (1991).

²B. Deveaud, J. Shah, T. C. Damen, B. Lambert, and A. Regreny, *Phys. Rev. Lett.* **58**, 2582 (1987); B. Deveaud, J. Shah, T. C. Damen, B. Lambert, A. Chomette, and A. Regreny, *IEEE J. Quantum Electron.* **24**, 1641 (1988) and references therein.

³D. F. Nelson, J. A. Cooper, and A. R. Tretola, *Appl. Phys. Lett.* **41**, 857 (1982).

⁴H. Hillmer, S. Hansmann, A. Forchel, M. Morohashi, E. Lopez, H. P. Meier, and K. Ploog, *Appl. Phys. Lett.* **53**, 1937 (1988).

⁵H. Hillmer, A. Forchel, S. Hansmann, M. Morohashi, E. Lopez, H. P. Meier, and K. Ploog, *Phys. Rev. B* **39**, 10 901 (1989).

⁶H. Hillmer, A. Forchel, S. Hansmann, E. Lopez, and G. Weimann, *Solid State Electron.* **31**, 485 (1988).

⁷H. Hillmer, A. Forchel, R. Sauer, and C. W. Tu, *Phys. Rev. B* **42**, 3220 (1990).

⁸H. Sakaki, T. Noda, K. Hirakawa, M. Tanaka, and T.

Matsusue, *Appl. Phys. Lett.* **51**, 1934 (1987), and references therein.

⁹R. Gottinger, A. Gold, G. Abstreiter, G. Weimann, and W. Schlapp, *Europhys. Lett.* **6**, 183 (1988); A. Gold, *Phys. Rev. B* **38**, 10 798 (1988).

¹⁰M. Wataya, H. Goto, N. Sawaki, and I. Akasaki, *Jpn. J. Appl. Phys.* **168**, 1934 (1989).

¹¹C. W. Tu, R. C. Miller, B. A. Wilson, P. M. Petroff, T. D. Harris, R. F. Kopf, S. K. Sputz, and M. C. Lamont, *J. Cryst. Growth* **81**, 159 (1987).

¹²G. Mahler, G. Maier, A. Forchel, B. Laurich, H. Sanwald, and W. Schmid, *Phys. Rev. Lett.* **47**, 1855 (1981); G. Mahler and A. Forchel, *Helv. Phys. Acta* **56**, 875 (1983).

¹³G. A. Northrop and J. P. Wolfe, *Phys. Rev. Lett.* **43**, 1424 (1979); M. Greenstein, M. A. Tamor, and J. P. Wolfe, *Phys. Rev. B* **26**, 5604 (1982).

¹⁴P. Lugli, *Solid State Electron.* **31**, 667 (1988).

¹⁵R. G. Ulbrich, V. Narayanamurti, and M. A. Chin, *J. Phys. (Paris)* **42**, C6-222 (1981).

¹⁶V. S. Bagaev, L. V. Keldysh, N. N. Sibel'din, and V. S. Tsetkov, *Zh. Eksp. Teor. Fiz.* **70**, 702 (1976) [*Sov. Phys. JETP* **43**, 362 (1976)].

¹⁷J. C. Hensel and R. C. Dynes, *Phys. Rev. Lett.* **43**, 1424 (1979).

¹⁸L. M. Smith, J. S. Preston, J. P. Wolfe, D. R. Wake, J. Klem, T. Henderson, and H. Morkoç, *Phys. Rev. B* **39**, 1862 (1989).

¹⁹K. Fujiwara (private communication).